Turner Simon (Orcid ID: 0000-0002-6426-6495)
Rushmer Tracy (Orcid ID: 0000-0003-0192-2384)

Lithium isotope variations in Tonga-Kermadec arc–Lau back-arc lavas and DSDP Site 204 sediments

Brens Jr., Raul [1], Liu, Xiao-Ming[2], Turner, Simon[1], Rushmer, Tracy[1]*

[1]Department of Earth and Planetary Sciences, Macquarie University, Sydney, NSW 2109, Australia
[2]Department of Geological Sciences, University of North Carolina, Chapel Hill, NC 27599, USA

This is the author manuscript accepted for publication and has undergone full peer review but has not been through the copyediting, typesetting, pagination and proofreading process, which may lead to differences between this version and the Version of Record. Please cite this article as doi: 10.1111/iar.12276

*Corresponding author: tracy.rushmer@mq.edu.au

Abstract

Lithium isotopes have been identified as a promising tracer of subducted materials in arc lavas due to the observable variations in related reserviors such as subducting sediments and altered oceanic crust. The Tonga-Kermadec arc–Lau back-arc provides an end-member of subduction zones with the coldest thermal structure on Earth. Reported here are Li isotope data for 14 lavas from the arc front and 7 back-arc lavas as well as 12 pelagic and volcaniclastic sediments along a profile through the sedimentary sequence at DSDP Site 204. The arc and back-arc lavas range from basalts to dacites in composition with SiO_2 = 48.3-65.3 wt% over which Li concentrations increase from 2 ppm to 16 ppm. Li/Y ratios range from 0.08 to 0.77 and from 0.24 to 0.65 in the arc and back-arc lavas, respectively. The majority of the lavas have δ^7Li that ranges from 2.5 ‰ to 5.0 ‰ with an average of (3.6 ±0.7) ‰, similar to that reported from other arcs and there is no distinction between the arc front and back-arc lavas. The pelagic sediments have variable Li concentrations (33–133 ppm) and δ^7Li that ranges from 1.2 ‰ to 10.2 ‰ whilst the volcaniclastic sediments have an even greater range of Li concentrations (3.6–165 ppm) and generally higher δ^7Li values (8–14 ‰). However, δ^7Li in the lavas does not correlate with commonly used trace element ratio or isotope signatures indicative of slab-derived fluids or the sediments. This is probably because the range of δ^7Li in the lavas and sediments overlap. Calculated sediment mass-balance models require significantly more sediment than previous estimates based on Th-Nd-Be isotopes. This may indicate that a sizeable proportion of the total Li budget in the lavas is provided by Li-enriched fluids from the subducting sediments and/or altered oceanic crust.

Keywords: DSDP 204 sediment profile; Lau back-arc; Li isotopes; Recycling Tonga-Kermadec arc

1 INTRODUCTION

Subduction recycles altered oceanic crust and overlying sediments into the mantle and there is much interest in the extent to which these components influence the composition of arc lavas and mantle that may much later be sampled at mid-ocean ridges and oceanic islands. Lithium is a light, fluid-mobile trace element that has also been widely evaluated as potential tracer of subduction zone recycling (Brenan, Ryerson, & Shaw, 1998; Caciagli, Brenan, McDonough, & Phinney, 2011; Elliott, Jeffcoate, & Bouman, 2004; Penniston-Dorland, Liu, & Rudnick, 2017; Ryan & Langmuir, 1987; Tang, Rudnick, & Chauvel, 2014; Tomascak 2004; Penniston-Dorland, Bebout, Pogge von Strandmann, Elliott, & Sorensen 2012; You, Castillo, Gieskes, Chan, & Spivac, 1996). The utility of Li isotopes in this regard reflects low temperature fractionation that occurs during weathering and the uptake of seawater into sediments and the altered oceanic crust (e.g. Brant et al., 2012; Chan, Edmond, Thompson, & Gillis, 1992; Gao et al., 2012; Liu, Wanner, Rudnick, & McDonough, 2015). Accordingly, Li isotope variations in mid-ocean ridge basalts have been taken as evidence for long-term "pollution" of the mantle by subducted components (Elliott, Thomas, Jeffcoate, & Niu, 2006) or local contamination in magma chambers (Tomascak, Langmuir, le Roux, & Shirey, 2008). Given this variation, it is disappointing that studies of arc lavas have frequently been frustrated by the lack of clear Li isotope signatures of subducted components and the ubiquitous range of $\delta^{7}Li = 3-4$ often being attributed to diffusive interaction between rising melts and the mantle wedge (e.g. Elliott et al., 2004; Tomascak, Widom, Benton, Goldstein, & Ryan, 2002). Nevertheless, some workers have found evidence for sediment-derived lithium isotope signals in arc lavas (Chan, Leeman, & You, 2002; Moriguti & Nakamura, 1998; Tang et al., 2014) and Plank (2014) has argued that the Li/Y ratios of arc lavas are actually dominated by sediment.

Finally, Magna, Wiechert, Grove, & Halliday (2006) and Kosler et al. (2009) have found evidence that back-arc lavas can have lower δ^7Li that their associated arc-front lavas.

In order to contribute to these on-going investigations, we present here Li concentration and isotope data from well-characterised samples from the oceanic Tonga-Kermadec arc and Lau back-arc as well as the sediment profile at DSDP Site 204 (Figure. 1). This arc encompasses the largest variation in subduction rates (6−24 cm/yr) worldwide (Bevis et al., 1995) and affords the opportunity to provide new insights into the debates outlined above because it erupts lavas which carry (1) a strong trace element (e.g. high Ba/Th, U/Th) fluid signature (Ewart, Collerson, Regelous, Wendt, & Niu, 1998; Turner et al., 1997), (2) very low HFSE concentrations indicative of a depleted wedge that is highly sensitive to slab contributions (Ewart et al., 1998; Turner et al.,1997), (3) ^{226}Ra evidence for rapid melt transport (Turner, Bourdon, Hawkesworth, & Evans, 2000), (4) ^{10}Be evidence for pelagic sediment addition (George et al., 2005), and (5) a unique tracer of subducted sediment as provided by the Louisville volocaniclastics (Regelous, Collerson, Ewart, & Wendt,1997; Turner et al., 1997). The back-arc lavas from the Fonualei Spreading Centre, the Mangatolo Triple Junction and Niuafo'ou offer a contrast to the arc front lavas because sediment- and fluid-related signatures become increasingly muted and the melting regime changes from fluid-fluxed to decompression dominated with increasing distance from the arc front (Caulfield, Turner, Dosseto, Pearson, & Beier, 2012). Our aims are to detail the Li isotope composition of the subducting sediment pile at DSDP Site 204, to use this to explore whether altered oceanic crust fluids and sediment singatures (especially that of the Louisville volcaniclastics) can be distinguished using Li isotopes and if so whether the back-arc lavas have a decreased subduction signature.

2 GEOLOGICAL SETTING AND SAMPLE DETAILS

The 2 800 km long Tonga-Kermadec island arc extends from the Taupo Volcanic Zone in New Zealand, to the Vitiaz strike-slip fault south of Samoa and results from subduction of the Pacific plate beneath the Australian plate (Figure 1). The arc is composed of more than 80 volcanoes, both above and below sea level (Stoffers et al., 2006; Wright, Worthington, & Gamble, 2006). The Louisville seamount chain, an aseismic ridge, intersects the arc, effectively splitting it into the Tonga segment to the north, and the Kermadec segment to the south. The subducting Pacific plate is 85−144 Ma old (Billen & Stock, 2000; Sutherland & Hollis, 2001) based on biostratigraphy of radiolarian chert and dating of ferrobasalts near to and from DSDP Holes 595/595A and 596/596A (Figure 1). Both the dip of the slab and the convergence rate increase from south to north. The plate dips at an angle of 30^{o} down to a depth of 20−130 km beneath both segments of the Tonga-Kermadec arc and steepens to 55−60^{o} in the Kermadec segment and 43−45^{o} in the Tonga segment (Isacks & Barazangi, 1977). Convergence rate along the Kermadec segment is 5 cm/yr, while in the Tonga segment the rate increases to 16−24 cm/yr (Bevis et al., 1995) implying a cold thermal structure (Syracuse, van Keken, & Abers, 2010) in which fluid contributions might be expected to dominate over those from the subducted sediments (e.g. Leeman, Tonarini, & Turner, 2017). The Tonga-Kermadec lavas consist predominantly of low-K basalts, basaltic andesites, andesites and minor dacites (see Ewart et al., 1998 for a summary).

The compositions of the sediments on the Pacific plate are well constrained and dominated by pelagic clays (Burns et al., 1973; Plank & Langmuir, 1998; Turner et al., 1997). Close to the Louisville Ridge these are underlain by volcaniclastics derived from this seamount chain. The thickness of sediment decreases northwards from 200 m to 70 m (Plank & Langmuir, 1998) and the lack of an accretionary prism suggests that the full sediment packet is subducted beneath this arc

(Bloomer & Fisher, 1986). Mass balance calculations show that only a minor amount (0.25−1 %) of the pelagic sediment is recycled into the lavas (George et al., 2005; Turner et al., 1997). Enrichment in $^{206}Pb/^{204}Pb$ is observed in the volcanoes at the northern end of the arc (Tafahi and Niuatoputapu), and this has been interpreted to reflect incorporation of the Louisville Ridge volcaniclastic sediments (Regelous,Gamble, & Turner, 2010; Turner, Handler, Bindeman, & Suzuki, 2009; Wendt, Regelous, Collerson, & Ewart, 1997).

Westward of the Tonga-Kermadec arc lie two active back-arc basins, the Havre Trough to the south, and the Lau Basin to the north. The rate of spreading increases northward from 6 cm/yr in the Havre Trough to 16 cm/yr in the northern Lau Basin (Bevis et al., 1995). In the northeast section of the Lau Basin the Fonualei Spreading Center (FSC) is an active spreading center that extends obliquely away from the active volcanic front northward to the Mangatolu Triple Junction (MTJ) and is punctuated by a series of transform faults that extend into the MTJ (Figure 1). The Lau back-arc basin basalts (BABB) range from near MORB-like compositions (Hawkins, 1995) when erupted far from the arc, to arc-like compositions when erupted close to the arc (Pearce et al., 1995). BABB, such as those erupted along the Fonualei Spreading Center and Valu Fa Ridge, show subduction signatures that are characterized by enrichments in LILE, volatile elements (e.g. they have up to 2.5 wt% H_2O), and show depletion in HFSE (Caulfield et al., 2012; Keller, Arculus, Hermann, & Richards, 2008; Langmuir, Bézos, Escrig, & Parman, 2013; Pearce & Stern, 2006).

The subaerial arc lavas analysed range from basalt to dacite in composition with SiO_2 = 48.3−65.3 wt% and include some pumiceous samples, while the submarine back-arc lavas are quenched glasses that range from basalt to basaltic andesite in composition. Full location, petrographic and geochemical data for all of these samples can be found elsewhere (Caulfield et al., 2012; Ewart & Hawkesworth, 1987; Ewart et al., 1998; George et al., 2005; Keller et al., 2008;

Leeman et al., 2017; Turner et al., 1997, 2000, 2009). For convience, we have provided the full geochemical data set in Supporting Information Table S1. We also analysed a boninite dredged from the north Tonga trench (Falloon & Crawford, 1991). The sediments samples come from DSDP Site 204 which has been subdivided into 3 units (Burns et al., 1973). Unit 1 comprises of pelagic clay and ash and dates from the Quaternary to early Miocene or Oligocene. Two samples analysed from the top of the clay unit are composed of dark brown clay that contains plagioclase (andesine), glass shards, mica, quartz, montmorillonite, zeolite, augite, and secondary clay phillipsite. Two samples from the bottom of the clay unit are dark reddish brown iron-oxide clay composed of montmorillonite, potash feldspar, quartz, amorphous iron oxide, glass shards, and some authigenic carbonate layers. The bottom two units are comprised of volcanogenic sediments derived from the Louisville Seamount Chain. Unit 2, from which three samples were analyzed, is a tuffaceous sandstone and conglomerate of early Cretaceous age. The clasts are composed of glass shards, andesine, calcite, pumice, and andesitic and basaltic rock fragments. The matrix is mainly altered ash with secondary minerals of epidote, zeolites, calcite, chloritic minerals, serpentine, and amorphous iron oxide. Unit 3, from which two samples were analyzed, is a vitric tuff composed of basaltic to andesitic glass with pyroxene and feldspar crystals in a glass matrix.

3 ANALYTICAL METHODS

The subaerial samples analysed were splits of powders for which major and trace element and radiogenic isotope data have been reported previously (Caulfield et al., 2012; Davidson, Turner, & Plank 2013; Ewart et al., 1998; Keller et al., 2008; Turner et al., 1997). The submarine glasses were rinsed in Milli-Q water to remove seawater (Keller et al., 2008). Both samples and standards were prepared for Li isotopic analysis at the University of Maryland by digesting the powders with a 3:1

mixture of concentrated HF and HNO_3 in Savillex® screw top beakers on a hot plate (T ~ 120 ^{o}C). This was followed by addition of concentrated HNO_3 and HCl, with drying between each stage of acid addition. The residue was then re-dissolved in 4 N HCl in preparation for chromatographic separation.

Lithium separation was achieved through ion-exchange chromatography, modified from Moriguti and Nakamura (1998), where four chromatographic columns were used. For each column, 1 mL of cation exchange resin of AG50w-X12, 200−400 mesh (Bio-Rad) was cleaned with HCl and Milli-Q water followed by conditioning, chemical separation and sample collection using an eluent mixture of HCl and ethanol. The first two columns remove major element cations with 2.5 M HCl and subsequently 0.15 M HCl. The third and fourth columns separate Na from Li with 30 % ethanol in 0.5 M HCl through a N_2 pressurized ion exchange column (Rudnick, Tomascak, Heather, & Gardner, 2004).

The samples were analyzed for ^{6}Li and ^{7}Li on a Nu Plasma multi-collector inductively coupled mass spectrometer (MC-ICP-MS) using Faraday cups. Li isotopic compositions were analyzed by bracketing the sample, before and after, with the L-SVEC standard. The δ^{7}Li value ($\delta^{7}Li = [[^{7}Li/^{6}Li]_{sample} / [^{7}Li/^{6}Li]_{standard} - 1 \times 1000]$) is expressed as per mil deviations from the L-SVEC standard (Flesch et al., 1973). External reproducibility of the isotopic compositions is d ±1.0 ‰ (2Ã) based on repeat runs of pure Li standard solutions: in-house standard UMD-1 (δ^{7}Li = 55.14 ‰, *n* = 5) and international standard reference material IRMM-016 (δ^{7}Li = 0.10 ‰, *n* = 5) (Liu, Rudnick, Hier-Majumder, & Sirbescu, 2010, Liu, Rudnick, McDonough, & Cummings, 2013; Teng, McDonough, Rudnick, Walker, & Sirbescu, 2006). The in-house and the international standard reference materials were analyzed at the beginning and end of each session and often a

third time between runs in which more than eight samples were analyzed. The amount of Li in proceedural blanks were negligible relative to the amounts extracted from the samples.

Lithium concentrations were determined by comparing sample signal intensities with those for the 50 ppb L-SVEC standard and then adjusting for sample weight. These measurements have a 2Ãuncertainty of d 10 % (Teng et al., 2006). Results for USGS international rock standards BHVO-2, AGV-2, and BCR-2 are reported in Table 1. The results are generally within analytical error of the recommended values from the U.S. Geological Survey and within the ranges for published data (Bouman, Elliott, & Vroon, 2004; Chan & Frey, 2003; Gladney & Goode, 1981; Govindaraju, 1994; James & Palmer, 2000; Liu et al., 2015; Penniston-Dorland et al., 2012; Ryan & Langmuir, 1987; Rudnick et al., 2004; Tang et al., 2014). The exception is BHVO-2 that produced values slightly higher than the accepted range of δ^7Li = (4.45 ±0.29) ‰ (Magna, Wiechert, & Halliday, 2004).

4 RESULTS

The new lava results are presented in Table 1 and the full dataset for these sampes including published data is provided as an Electronic Supplement. They have Li concentrations that range from 2 ppm to 16 ppm and overlap the global arc array on Figure 2a. Li/Y ratios range from 0.08 to 0.77 and from 0.24 to 0.65 in the arc and back-arc lavas, respectively (Figure 2b). As a moderately incompatible element Li concentrations increase with increasing SiO_2 (Figure 2a) but there is no clear correlation between δ^7Li and SiO_2 (Figure 2c). The majority of the lavas have δ^7Li that ranges from 2.5 ‰ to 5.0 ‰ with an average of (3.6 ±0.7) ‰ that is similar to those reported from other arcs (Bouman, Elliott, & Vroon, 2004; Moriguti & Nakamura, 1998; Tang et al., 2014; Tomasack, 2002; Tomascak, Ryan, & Defant, 2000). There are three lavas that lie outside of this range:

Niuatoputapu, 'Ata and L'Esperance. For the former two we replicated the data: Niuatoputapu with δ^7Li = 6.4 ‰ and 7.9 ‰, Ata with δ^7Li = 1.6 ‰ and 1.9 ‰. Unfortunately, there was insufficient powder from the L'Esperance sample to undertake a replicate analysis (δ^7Li = 0.3 ‰, see Table 1). Nevertheless, it appears that the range of δ^7Li in this arc can be slightly larger than those reported elsewhere (see Figure 2c and discussion below). The back-arc lavas cluster at the low Li, low SiO_2 end of the arrays on Figure 2a and overlap the median δ^7Li ratio of the arc lavas (Figure 2c). Whilst we cannot unambiguously rule out the effects of alteration we have to reason to suspect this is a significant problem.

The sediment profile at DSDP site 204 is presented in Table 2 and consists of ~ 100 m of pelagic sediments underlain by volcaniclastic sediments from the Louisville seamount chain (Burns et al., 1973). The pelagic sediments have quite variable Li concentrations (33−133 ppm) and δ^7Li that ranges from 1.2 ‰ to 10.2 ‰ (Figure 3a,c) similar to equivalent pelagic sediments analysed by Chan, Leeman, and Plank (2006) from DSDP Site 596 further to the east of the trench (see Figure 1). A concentration- and thickness-weighted average δ^7Li of the pelagic sediments at DSDP site 204 is 5.0 ‰. This and the overall the range lie within the data reported previously from a wide range of marine sediments (Chan et al., 2006). However, it is significantly heavier than the (3.4 ±1.4) ‰ value inferred for the depleted mantle (Tomascak et al., 2008) or sediment columns in the Lesser Antilles (δ^7Li = −0.4 ‰) or Sunda arcs (δ^7Li = +0.3 ‰) which are domiated by terrigenous phases (values taken from Plank, 2014). In comparison with the pelagic sediments, the volcaniclastic sediments at DSDP site 204 have a greater range of Li concentrations (3.6−165 ppm) and generally higher δ^7Li values of 8−14 ‰ (see Figure 3a,c). If these are included, the weighted average δ^7Li for at DSDP site 204 increases to 6.1 ‰. This lies toward the heavier end of the range of the bulk composition of subducting sedimentary columns calculated by Plank (2014). Li/Y ratios

of the sediment range from 0.2 to 8.6 (data from George et al., 2005). It must be emphasised that there are only 12 sediment samples and so we plot the fields for the sediments, as well as the weighted averages, on the figures. As shown on Figure 4, δ^{7}Li is lowest in the southern end of the arc and reaches its highest values in the northern end of the arc where the Louisville component was originally identified (see further discussion below).

5 DISCUSSION

In the following sub-sections we first assess the possible significance of the outlier lavas and then explore possible links to independent tracers of subducted components. As discussed elsewhere, there is good evidence (e.g. no correalted changes in radiogenic isotopes and indices of differentiation) that these lavas have not suffered from crustal contamination (Turner et al., 2009).

5.1 Lava and sediment data in the context of global observations

As shown on Figure 2, the lavas broadly overlap the global arc array in terms of both Li concentrations as well as Li/Y and δ^{7}Li. It is also clear from Figure 2 (and all subsequent figures) that there is no distinction between the arc-front and back-arc lavas in terms of δ^{7}Li unlike those from the Antarctic Peninsula or the Cascades (Leeman, Tonarini, Chan, & Borg, 2004; Magna et al., 2006; Kosler et al., 2009) where the back-arc lavas have lower δ^{7}Li than the arc front. As discussed by Plank (2014), most arc lavas have Li/Y ratios greater than that of MORB (Li/Y = 0.2, Ryan & Langmuir, 1987) and the average Li/Y for a large number of arcs (including Tonga) correlates well with the Li/Y ratio of the local bulk subducting sediment. Thus, the elevated Li/Y ratios are most readily explained by sediment addition yet the majority of arc lavas perplexingly fall within the range of δ^{7}Li in MORB (Tomascak et al., 2008). This reasoning is equally valid for most

of our new data from Tonga-Kermadec with the exception of Niuatoputapu, 'Ata and L'Esperance (Figure 2b,c).

The DSDP Site 204 sediments become broadly heavier in δ^7Li with increasing depth (Figure 3b) and a weighted avreage of the entire DSDP Site 204 column falls at the higher end of sediment values globally (see Plank, 2014). Thus, the elevated δ^7Li value of the Niuatoputapu lava could be explained by addition of a Louisville volcaniclastic component and this island lies at the northern end of the arc (see Figures 1 and 4) where this signature is believed to have been stored in the lithosphere for several Myr (Beier et al., 2017; Regelous et al., 1997; Turner et al., 1997). However, it is unclear why an equivalent signature is not observed in the Tafahi lava since both carry the elevated $^{206}Pb/^{204}Pb$ Louisville signature. The 'Ata sample lies just below the δ^7Li range for MORB and we note that both B and Pb isotope signature of lavas from this island are atypical of the rest of the central Tongan islands (Ewart et al., 1998; Leeman et al., 2017). Finally, the very low δ^7Li ratio from the L'Esperance lava may regretably reflect alteration since this sample has a high chemical index of alteration (Nesbitt & Young, 1982) of 64 compared to the other lavas (48−58).

5.2 Controls on Li isotopic composition

Many studies have utilized U/Th and Th/Ce ratios as tracers of fluid and sediment components in arc lavas (e.g. Plank & Langmuir, 1998; Turner et al., 1997). On Figure 5a we plot δ^7Li against U/Th as a tracer of fluid contributions from the subducting plate. Overall there is a weak positive correlation but the majority of the lavas lie between likely average compositions of the mantle wedge (DMM) and altered oceanic crust (AOC) which can have a very large range in δ^7Li (Gao et al., 2012). Here the Niuatoputapu lava is clearly displaced from the remaining lavas towards the average volcaniclastic sediment composition. No correlation is observed when the δ^7Li data from

the Tonga-Kermadec lavas are plotted against indices of sediment addition such as Th/Ce (Figure 5b) unlike the findings of Moriguti and Nakamura (1998) or Chan et al. (2002). The back-arc lavas lie at the low U/Th, low Th/Ce end of the data, consistent with lesser overall contributions from the slab (Caulfield et al., 2012) but this distinction is not evident in $\acute{}^{7}$Li.

On Figure 6 we investigate variations between $\acute{}^{7}$Li and two other isotope systems that tend to track sub-arc fluid additions since both B and Sr are fluid mobile (Brenan et al., 1998). There is no correlation between $\acute{}^{7}$Li and $^{87}Sr/^{86}Sr$ though, as on Figure 5a, both the arc front and back-arc lavas fall broadly between DMM and AOC and the average sediment compositions. Although there are fewer data, we plot $\acute{}^{7}$Li versus δ^{11}B on Figure 6b. Once again, there is no correlation though the diagram does highlight the unusually light B in the 'Ata sample that may reflect complex mantle wedge circulation caused by the locus of present day subduction of the Louisville seamounts (see also Leeman et al., 2017) but it most clearly does not carry a Louisville $\acute{}^{7}$Li signature. This casts doubt on the hypothesis that the elevated $^{206}Pb/^{204}Pb$ obeserved in some seamounts just to the north of 'Ata (e.g. Monowai) are derived from the Louisville Ridge (Timm, Graham, de Ronde, Leybourne, & Woodhead, 2011).

Unfortunately, the conclusion from Figures 5 and 6 (and equivalent diagrams not shown) has to be that there are no observations with respect to $\acute{}^{7}$Li that unambiguously distinguish between sediment and fluid addition as the main control on the variations in $\acute{}^{7}$Li in the Tonga-Kermadec-Lau lavas. It is possible that diffusive equilibration with non-subduction modified mantle wedge has erased much of any putative initial subduction-derived signatures (e.g. Elliott et al., 2004; Penniston-Dorland et al., 2012). However, the elevated Li/Y ratios seem to require sediment addition and Tonga lies on the correlation between the average Li/Y of the lavas and the Li/Y ratio of the local bulk subducting sediment (Plank, 2014). Rather, it may be that the sediment signal is

not clear in δ^{7}Li becasuse the Li isotope composition of the lavas largely overlap those of the local subducting sediments. This constrasts with systems like the Lesser Antilles arc where the sediment has particularly light δ^{7}Li that can be observed to influence the local lavas (Tang et al., 2014). Moreover, at least one robust sediment δ^{7}Li signal exists in case of the Louisville volcaniclastic signature observed in the lava from Niuatoputapu, although it is unclear why this is not observed in lavas from the neighbouring island of Tafahi.

5.3 Quantification of sediment mixing

Given the Li/Y argument for sediment addition, the volcaniclastic sediment singal at Niuatoputapu and unambiguous evidence from the presence of live ^{10}Be in the lavas (George et al., 2005) we assessed an end-member model in which all of the δ^{7}Li–Li/Y variation is assumed to reflect bulk sediment addition (Figure 7). This is shown on a plot of δ^{7}Li versus Y/Li (ratio inverted so that mixing is linear) overlain on the results of a Monte Carlo simulation involving bulk sediment addition to a mantle wedge that had been previsouly depleted by 1 % melt extraction (Caulfield et al., 2008). The simulation allows the full range of sediment compositions from Table 2 to be involved. Given the overlapping range in δ^{7}Li in the lavas and local sediments it is perhaps an unsurprising outcome that the resultant envelope of solutions encompasses the full variation observed in the lavas (see Figure 7). However, the implied amounts of sediment addition required (1–3 %) exceed, significantly, those estimated (0.1–0.5 %) on the basis of Th-Nd-Be isotopes (George et al., 2005; Turner et al., 1997). This may best be explained by the highly fluid-mobile nature of Li (e.g. Brenan et al., 1998; Caciagli et al., 2011; Johnson & Plank, 1999; Kessel, Schmidt, Ulmer, & Pettke, 2005) with the implication that fluid scavenging of Li from the sediments may have played a significant role in controlling the Li isotope variations. In otherwords,

preconcentration of Li by fluid mobilisation of sedimentary Li would decrease the inferred amount of sediment addition on Figure 7. This can simlutaneously explain the elevated Li/Y ratios since Li and Y partition similarly during mantle partial melting (Ryan & Langmuir, 1987). Although we accept that three-component models will necessarily be non-unique, Leeman et al. (2017) have recently argued that, because the Tonga slab lies at the cold end of the global thermal structure spectrum (Syracuse et al. 2010), fluid addition (from both sediments and AOC) may be the principle means of slab-derived element transport beneath this arc. The relationships on Figures 5 and 6 are not inconsistent with such models from a Li isotope perspective. Further development will require better knowledge of when and at what temperatures fluids are driven off the sediments and AOC of the slab.

6 CONCLUSIONS

We have undertaken a reconnaissance study of Li isotopes in the oceanic Tonga-Kermadec arc and Lau back-arc as well as the sediment profile at DSDP Site 204. Unfortunately, despite being an end-member arc in terms of cold thermal structure and having an unique sediment tracer in the Louisville volcaniclastics, there is no clear discernment of sediment or fluid contributions with respect to Li isotopes even though elevated Li/Y ratios would appear to demand a sediment contribution. The exception is one lava from Niuatoputapu Island that appears to carry a signature from the subducting Louisville volcaniclastic sediments. Lavas from ‘Ata and L’Esperance Islands have unusually low δ^{7}Li of unknown origin. The remaining arc front and back-arc lavas overlap with δ^{7}Li = (3.6 ±0.7) 0 . Modelled δ^{7}Li–Y/Li relationships require 1–3 % bulk sediment addition to explain the range in observed ratios. This is significantly higher than suggested by previsouly

published Th-Nd-Be isotope systematics and may implicate an important role for fluid scavenging of Li from the subducting sediments (and altered oceanic crust) beneath this arc–back-arc system.

ACKNOWLEDGMENTS

R.B. thanks Richard Ash for the help he provided in the plasma lab and Ming Tang for helping facilitate samples between the US and Australia. We grateful to Juan-Carlos Afonso for performing the Monte Carlo simulation. Our work was supported by a PhD stipend from Macquarie University, the NSF Grant EAR 0948549 to Roberta Rudnick and Bill McDonough and the sediment core samples were provided by IODP. Bill Leeman and an anonomous reviewer provided helpful comments on the the manuscript.

REFERENCES

Bevis, M., Taylor, F. W., Schutz, B. E., Recy, J., Isacks, B. L., Helu, S., ..., Stowell, J. (1995). Geodetic observations of very rapid convergence and back-arc extension at the Tonga arc. *Nature*, *374*, 249–251.

Beier, C., Turner, S., Haase, K.M., Pearce, J., Munker, C., & Regelous, M. (2017). Trace element and isotope geochemistry of the northern and central Tongan islands with an emphasis on the genesis of high Nb/Ta signatures at the northern volcanoes of Tafahi and Niuatoputapu. *Journal of Petrology*, *58*, 1073–1106.

Billen, M. I., & Stock, J. (2000). Morphology and origin of the Osbourn Trough. *Journal of Geophysics Research*, *105*, 13481–13489.

Bloomer, S. H., & Fisher, R. L. (1986). Petrology and geochemistry of igneous rocks from the Tonga trench – A non-accreting plate boundary. *Journal of Geology*, *95*, 469–495.

Bouman, C., Elliott, T., & Vroon, P. Z. (2004). Lithium inputs to subduction zones. *Chemical Geology*, *212*, 59–79.

Brant, C., Coogan, L. A., Gillis, K. M., Seyfried, W. E., Pester, N. J., & Spence, J. (2012). Lithium and Li-isotopes in young altered upper oceanic crust from the East Pacific Rise. *Geochimica et Cosmochimica Acta*, *96*, 272–293.

Brenan, J. M., Ryerson, F. J., & Shaw, H. F. (1998). The role of aqueous fluids in the slab-to-mantle transfer of boron, beryllium, and lithium during subduction; experiments and models. *Geochimica et Cosmochimica Acta*, *62*, 337–3347.

Burns, R. E., Andrews, J. E., van der Lingen, G. J., Churkin, M., Jr., Galehouse, J. S., Packham, G., ..., Von Herzen, R. P. (1973). Site 204. *Initial Reports of the Deep Sea Drilling Project*, *21*, 33–56.

Caciagli, N., Brenan, J. M., McDonough, W. F., & Phinney, D. (2011). Mineral–fluid partitioning of lithium and implications for slab–mantle interaction. *Chemical Geology*, *280*, 384–398.

Caulfield, J. T., Turner, S., Dosseto, A., Pearson, N. J., & Beier, C. (2008). Source depletion versus extent of melting in the Tongan sub-arc mantle. *Earth and Planetary Science Letters*, *273*, 279–288.

Caulfield, J., Turner, S., Arculus, R., Dale, C., Jenner, F., Pearce, J., ..., Handley, H. (2012). Mantle flow, volatiles, slab-surface temperatures and melting dynamics in the north Tonga arc–Lau back-arc basin. *Journal of Geophysical Research: Solid Earth*, *B11209*, 1–17.

Chan, L. H., & Frey, F. A. (2003). Lithium isotope geochemistry of the Hawaiian plume: results from the Hawaii Scientific Drilling Project and Koolau Volcano. *Geochemistry, Geophysics, Geosystems*, *4*, 8707.

Chan, L. H., Edmond, J. M., Thompson, G., & Gillis, K. (1992). Lithium isotopic composition of submarine basalts; implications for the lithium cycle in the oceans. *Earth and Planetary Science Letters*, *108*,151–160.

Chan, L. H., Leeman, W. P., & You, C. F. (2002). Lithium isotopic composition of Central American Volcanic Arc lavas: Implications for modification of the subarc mantle by slab-derived fluids: Correction. *Chemical Geology*, *182*, 293–300.

Chan, L. H., Leeman, W. P., & Plank, T. (2006). Lithium isotopic composition of marine sediments. *Geochemistry, Geophysics, Geosystems*, *7*, Q06005.

Davidson, J., Turner, S., & Plank, T (2010). Dy/Dy*: variations arising from mantle sources and petrogenetic processses. *Journal of Petrology*, *54*, 525–537.

Elliott, T., Jeffcoate, A., & Bouman, C. (2004). The terrestrial Li isotope cycle: light-weight constraints on mantle convection. *Earth and Planetary Science Letters*, *220*, 231–245.

Elliott, T., Thomas, A., Jeffcoate, A., & Niu, Y. (2006). Lithium isotope evidence for subduction-enriched mantle in the sources of mid-ocean ridge basalts. *Nature*, *443*, 565–568.

Ewart, A., & Hawkesworth, C. J. (1987). The Pleistocene-Recent Tongan-Kermadec arc lavas: interpretation of new isotope and rare earth data in terms of a depleted mantle source model. *Journal of Petrology*, *28*, 295–330.

Ewart, A., Collerson, K. D., Regelous, M., Wendt, J.I ., & Niu, Y. (1998). Geochemical evolution within the Tonga-Kermadec-Lau arc-back-arc systems; the role of varying mantle wedge composition in space and time. *Journal of Petrology*, *39*, 31–368.

Falloon, T. J., & Crawford, A. J. (1991). The petrogenesis of high-calcium boninite lavas dredged from the northern Tonga ridge. *Earth and Planetary Science Letters*, *102*, 375–394.

Flesch, G., Anderson, A. R., & Svec, H. J. (1973). A secondary isotopic standard for $^{6}Li/^{7}Li$ determinations. *International Journal of Mass Spectrometry and Ion Physics*, *12*, 265–272.

Gao, Y., Vils, F., Cooper, K. M., Banerjee, N., Harris, M., Hoefs, J., …Muechlenbachs, K. (2012). Downhole variation of lithium and oxygen isotopic compositions of oceanic crust at East Pacific Rise, ODP Site 1256. *Geochemistry, Geophysics, Geosystems, 13*,1–24.

George, R., Turner, S., Morris, J., Plank, T., Hawkesworth, C.J., & Ryan, J. (2005). Pressure-temperature-time paths of sediment recycling beneath the Tonga-Kermadec arc. *Earth and Planetary Science Letters*, *233*, 195–211.

Gladney, E. S., & Goode, W. E. (1981). Elemental concentrations in eight new United States Geological Survey rock standard: a review. *Geostandards Newsletter*, *5*, 31–64.

Govindaraju, K. (1994). Compilation of working values and sample descriptions for 383 geostandards. *Geostandards Newsletter*, *5*, 31–64.

Hawkins, J. W. (1995). The geology of the Lau Basin. In B. Taylor (Ed) *In Backarc Basins: Tectonics and Magmatism* (pp. 63–138), New York, USA, Plenum Press.

Isacks, B. L., & Barazangi, M. (1977). Geometry of Benioff zones: Lateral segmentation and downwards bending of the subducted lithosphere. In: *Island Arcs Deep Sea Trenches and Back-Arc Basins* (pp. 99–114), Maurice Ewing Ser. 1,

James, R. H., & Palmer, M. R. (2000). The Li isotope composition of international rock standards. *Chemical Geology*, *166*, 319–326.

Johnson, M. C., & Plank, T. (1999). Dehydration and melting experiments constrain the fate of subducted sediments. *Geochemistry, Geophysics, Geosystems*, *1*, 1–26.

Keller, N. S., Arculus, R. J., Hermann, J., & Richards, S. (2008). Submarine back-arc lava with arc signature: Fonualei Spreading Center, northeast Lau Basin, Tonga. *Journal of Geophysical Research*, *113*, 1–28.

Kelley, K. A., Plank, T., Ludden, J., & Staudigel, H. (2003). Composition of altered oceanic crust at ODP Sites 801 and 1149. *Geochemistry, Geophysics, Geosystems*, *4*, 1–21.

Kessel, R., Schmidt, M. W., Ulmer, P., & Pettke, T. (2005). Trace element signature of subduction-zone fluids, melts and supercritical liquids at 120–180 km depth. *Nature*, *437*, 724–727.

Kosler, J., Magna, T., Mlcoch, B., Mixa, P., Nyvlt, D., & Holub, F. V. (2009). Combined Sr, Nd, Pb and Li isotope geochemistry of alkaline lavas from northern James Ross Island (Antarctic Peninsula) and implications for back-arc magma formation. *Chemical Geology*, *258*, 207–218.

Langmuir, C. H., Bézos, A., Escrig, S., & Parman, S. W. (2013). Chemical Systematics and Hydrous Melting of the Mantle in Back-Arc Basins. In D. M. Christie, C. R. Fisher, S.-M. Lee and S. Givens (Eds.), *Back-Arc Spreading Systems: Geological, Biological, Chemical, and Physical Interactions* (pp 87-146. Washington, D. C., USA American Geophysical Union.

Leeman, W. P., Tonarini, S., Chan, L. H., & Borg, L. E. (2004). Boron and lithium isotopic variations in a hot subduction zone – the southern Washington Cascades. *Chemical Geology*, *212*, 101–124.

Leeman, W. P., Tonarini, S., & Turner, S. (2017). Boron isotope variations in Tonga-Kermadec-New Zealand arc lavas: implications for origin of subduction components and mantle influences. *Geochemistry, Geophysics, Geosystems*, *18*, 1126–1162.

Liu, X. M., & Rudnick, R. L. (2011). Constraints on continental crustal mass loss via chemical weathering using lithium and its isotopes. *Proceedings of the National Academy of Sciences of the United States of America*, *108*, 20873–20880.

Liu, X. M., Rudnick, R. L., Hier-Majumder, S., & Sirbescu, M. C. (2010). Processes controlling lithium isotopic distribution in contact aureoles; a case study of the Florence County pegmatites, Wisconsin. *Geochemistry, Geophysics, Geosystems*, *11*, 1–21.

Liu, X. M., Rudnick, R. L., McDonough, W. F., & Cummings, M. L. (2013). Influence of chemical weathering on the composition of the continental crust; insights from Li and Nd isotopes in bauxite profiles developed on Columbia River basalts. *Geochimica et Cosmochimica Acta*, *115*, 73–91.

Liu, X. M., Wanner, C., Rudnick, R. L., & McDonough, W. F. (2015). Processes controlling δ^{7}Li in rivers illuminated by study of streams and groundwaters draining basalts. *Earth and Planetary Science Letters*, *409*, 212–224.

Magna, T., Wiechert, U. H., & Halliday, A. N. (2004). Low-blank isotope ratio measurement of small samples of lithium using multiple-collector ICPMS. *International Journal of Mass Spectrometry*, *239*, 67–76.

Magna, T., Wiechert, U. H., Grove, T. L., & Halliday, A. N. (2006). Lithium isotope fractionation in the southern Cascadia subduction zone. *Earth and Planetary Science Letters*, *250*, 428–443.

Moriguti, T., & Nakamura, E. (1998). Across-arc variation of Li isotopes in lavas and implications for crust/mantle recycling at subduction zones. *Earth and Planetary Science Letters*, *163*, 167–174.

Nesbitt, H. W., & Young, G. M. (1982). Early Proterozoic climates and plate motions inferred from the major element chemistry of lutites. *Nature*, *299*, 715–717.

Pearce, J. A., & Stern, R. J. (2006). Origin of back-arc basin magmas; trace element and isotope perspectives. *Geophysical Monograph*, *166*, 63–86.

Pearce, J. A., Ernewein, M., Bloomer, S. H., Parson, L. M., Murton, B. J., & Johnson, L.E. (1995). Geochemistry of Lau Basin volcanic rocks: Influence of ridge segmentation and arc proximity. In J. L. Smellie (Ed.), *Volcanism Associated With Extension at Consuming Plate Margins*, (pp. 21–27) London, UK, Geological Society Special Publications 81.

Penniston-Dorland, S. C., Bebout, G. E., Pogge von Strandmann, P. A., Elliott, T., & Sorensen, S. S. (2012). Lithium and its isotopes as tracers of subduction zone fluids and metasomatic processes: Evidence from the Catalina Schist, California, USA. *Geochimica et Cosmochimica Acta*, *77*, 530–545.

Penniston-Dorland, S., Liu, X.-M., & Rudnick, R. L. (2017). Lithium isotope geochemistry. *Reviews in Mineralogy and Geochemistry*, *82*, 165–217.

Plank, T., & Langmuir, C. H. (1998). The chemical composition of subducting sediment and its consequences for the crust and mantle. *Chemical Geology*, *145*, 325–394.

Plank, T. (2014). The chemical composition of subducting sediments. *Treatise on Geochemistry*, 2nd Edition, Elsevier, http://dx.doi.org/10.1016/B978-0-08-095975-7.00319-3.

Regelous, M., Collerson, K. D., Ewart, A., & Wendt, J. I. (1997). Trace element transport rates in subduction zones; evidence from Th, Sr and Pb isotope data for Tonga-Kermadec Arc lavas. *Earth and Planetary Science Letters*, *150*, 291–302.

Regelous, M., Gamble, J. A., & Turner, S. P. (2010). Mechanism and timing of Pb transport from subducted oceanic crust and sediment to the mantle source of arc lavas. *Chemical Geology*, *273*, 46–54.

Rudnick, R. L., Tomascak, P.B., Heather, B. N., & Gardner, L.R. (2004). Extreme lithium isotopic fractionation during continental weathering revealed in saprolites from South Carolina. *Chemical Geology*, *212*, 45–57.

Ryan, J. G., & Langmuir, C. H. (1987) The systematics of lithium abundance in young volcanic rocks. *Geochimica et Cosmochimica Acta*, *51*, 1727–1741.

Salters, V. J. M., & Stracke, A. (2004). Composition of the depleted mantle. *Geochemistry, Geophysics, Geosystems, 5*, 1–27.

Stoffers, P., Worthington, T. J., Schwarz-Schampera, U., Hannington, M. D., Massoth, G. J., Hekinian, R., ..., Kerby, T. (2006). Submarine volcanoes and high-temperature hydrothermal venting on the Tonga arc, southwest Pacific. *Geology*, *34*, 453–456.

Sutherland, R., & Hollis, C. (2001). Cretaceous demise of the Moa plate and strike-slip motion at the Gondwana margin. *Geology*, *29*, 279–282 .

Syracuse, E. M., van Keken, P. E., & Abers, G. A. (2010). The global range of subduction zone thermal models. *Physics of the Earth and Planetary Interiors*, *183*, 73–90.

Tang, M., Rudnick, R. L., & Chauvel, C. (2014). Sedimentary input to the source of Lesser Antilles lavas: A Li perspective. *Geochimica et Cosmochimica Acta*, *144*, 43–58.

Teng, F. Z., McDonough, W. F., Rudnick. R. L., Walker, R. J., & Sirbescu, M. L. C. (2006). Lithium isotopic systematics of granites and pegmatites from the Black Hills, South Dakota. *American Mineralogist*, *91*, 1488–1498.

Timm, C., Graham, I. J., de Ronde, C. E. J., Leybourne, M. I., & Woodhead, J. (2011). Geochemical evolution of Monowai volcanic center: New insights into the northern Kermadec arc subduction system, SW Pacific. *Geochemistry, Geophysics, Geosystems*, *12*, 1–20.

Tomascak, P. B. (2004). Developments in the understanding and application of Lithium isotopes in the Earth and Planetary Sciences. *Reviews in Mineralogy and Geochemistry*, *55*, 153–195.

Tomascak, P. B., Ryan, J. G., & Defant, M. J. (2000). Lithium isotope evidence for light element decoupling in the Panama subarc mantle. *Geology*, *28*, 507–510.

Tomascak, P. B., Widom, E., Benton, L. D., Goldstein, S. L., & Ryan, J. G. (2002). The control of lithium budgets in island arcs. *Earth and Planetary Science Letters*, *196*, 227–238.

Tomascak, P. B., Langmuir, C. H., le Roux, P. J., & Shirey, S. B. (2008). Lithium isotopes in global mid-ocean ridge basalts. *Geochimica et Cosmochimica Acta*, *72*, 1626-–1637.

Turner, S., Hawkesworth, C., Rogers, N., Bartlett, J., Worthington, T., Hergt, J., ..., Smith, I. (1997). ^{238}U- ^{230}Th disequilibria, magma petrogenesis, and flux rates beneath the depleted Tonga-Kermadec island arc. *Geochimica et Cosmochimica Acta*, *61*, 4855–4884.

Turner, S., Bourdon, B., Hawkesworth, C., & Evans, P., (2000). ^{226}Ra-^{230}Th evidence for multiple dehydration events, rapid melt ascent and the time scales of differentiation beneath the Tonga-Kermadec island arc. *Earth and Planetary Science Letters*, *179*, 581–593.

Turner, S., Handler, M., Bindeman, I., & Suzuki, K. (2009). New insights into the origin of O-Hf-Os isotope signatures in arc lavas from Tonga-Kermadec. *Chemical Geology*, *266*, 196–202.

Wendt, J. I., Regelous, M., Collerson, K. D., & Ewart, A. (1997). Evidence for a contribution from two mantle plumes to island-arc lavas from northern Tonga. *Geology*, *25*, 611–614.

Wright, I. C., Worthington, T. J., & Gamble, J. A. (2006). New multibeam mapping and geochemistry of the 30–35 S sector, and overview, of southern Kermadec arc volcanism. *Journal of Volcanology and Geothermal Research*, *149*, 263–296.

You, C. F., Castillo, P. R., Gieskes, J. M., Chan, L. H., & Spivac A. J. (1996). Trace element behavior in hydrothermal experiments: Implications for fluid processes at shallow depths in subduction zones. *Earth and Planetary Science Letters*, *140*, 41–52.

A list of Supporting Information:

TABLE S1. Full geochemical data set for the samples used in this study

FIGURE 1. Map of the Tonga-Kermadec arc–Lau back-arc region showing the localities of the samples analysed. Also shown are the DSDP Sites 204 and 596. ELSC, Eastern Lau Spreading Centre; FSC, Fonualei Spreading Centre; MTJ, Mangatolo Triple Junction; VFSC, Valu Fa Spreading Centre

FIGURE 2. These plots present Li concentration versus Li/Y, Li concentration versus δ^7Li and Li concentration versus SiO_2 for the Tonga-Kermadec-Lau lavas. (a) shows Li concetration versus Li/Y, (b) shows Li concentration versus δ^7Li, and (c) shows Li concentrationa versus SiO_2. The average compositions of the DSDP Site 204 pelagic (+) and volcaniclastic (x) sediments are also shown as well as the fields for the sediments. Small grey circles are literature data for lavas from other arcs (Moriguti & Nakamura, 1998; Tang et al., 2014; Tomascak et al., 2000, 2002). Arrow indicates the Li/Y ratio of MORB on (b) and dashed lines on (c) indicate the range of normal MORB (Tomascak et al., 2008).

FIGURE 3. These profiles present Li concentration versus δ^7Li and Li concentration versus depth in the subducting sediment sequence. (a) shows Li concentration versus δ^7Li and (b) shows Li concentration versus depth. The crosses are DSDP Site 204 data from Table 2 and the grey circles are pelagic sediments from DSDP Site 596 (Chan et al., 2006). Note that the Louisville volcaniclastic sediments of Units 2 and 3 at Site 204, that include some of the highest Li concentrations and δ^7Li values, are not present at Site 596.

FIGURE 4. Plot of δ^7Li ‰ versus southern latitude. The occurrence of the elevated value δ^7Li in the Niuatoputapu lava at the northern end of the arc may reflect addition of a Louisville volcaniclastic component to the source of the lavas here (Regelous et al., 1997; Turner et al., 1997).

Figure 5. These plots show of δ^7Li versus U/Th, as a fluid-sensitive index, and δ^7Li versus Th/Ce as a sediment-sensitive index. (a) shows δ^7Li versus U/Th (b) shows δ^7Li versus Th/Ce. In (a) there is a weak positive correlation with U/Th if Niuatoputapu is ignored and for (b) it should be noted that only two sediments have been analysed for both B and Li isotopes. The average compositions of the DSDP Site 204 pelagic and volcaniclastic sediments are also shown as well as the fields for the sediments and average estimates for depleted MORB mantle (DMM) and altered oceanic crust (AOC): data from Elliott et al. (2004), Gao et al. (2012), Kelley, Plank, Ludden, & Staudigel, (2003), Salters &Stracke (2004).

FIGURE 6. Plot of δ^7Li versus $^{87}Sr/^{86}Sr$ and δ^7Li versus δ^{11}B. (a) shows δ^7Li versus $^{87}Sr/^{86}Sr$ and (b) shows δ^7Li versus δ^{11}B. Boron isotope data from Leeman et al. (2017), other symbols and data sources as for Figure 4.

FIGURE 7. Plot of δ^7Li versus Y/Li to appraise the potential of addition of bulk sediment to a depleted mantle source (DMM-1 %) to explain the range of δ^7Li in the Tonga-Kermadec-Lau lavas. The gradation of colour in the background represents random mixing results using a Monte Carlo simulation, the bar to the right represents the amount of sediment (%) required to attain that value in the simulation (small coloured circles are the analysed sediments that fall within the Monte Carlo

envelope). The DMM-1 % source has Li = 0.7 ppm, Y = 4.1 ppm and ′ ^{7}Li = +3.4 ‰ (Tomascak et al., 2008). See text for discussion. Note that although the 3 dacites are included their Y/Li may have become slightly increased during fractionation (cf. Figure 2b).

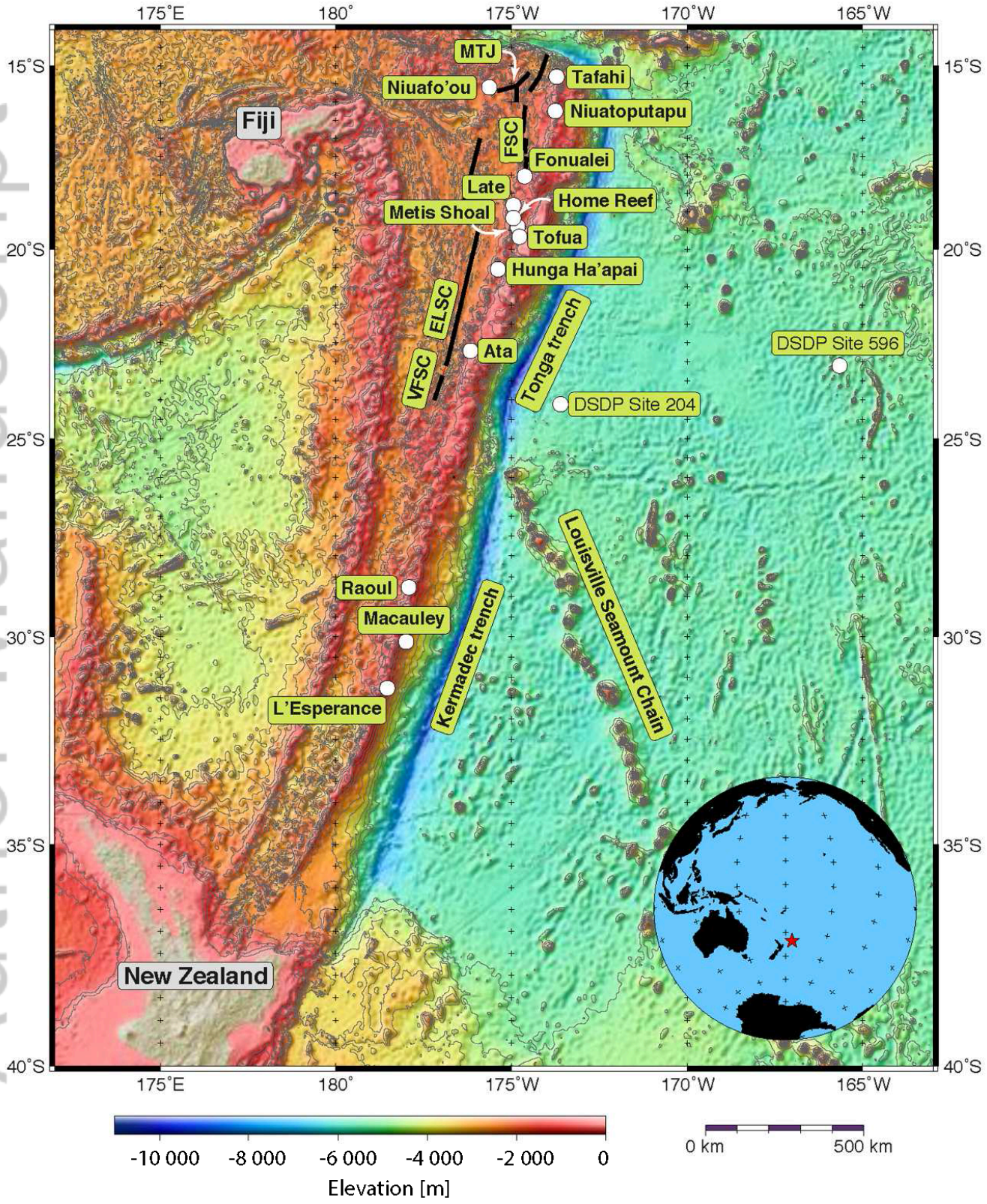

IslandArc_Figure1.png

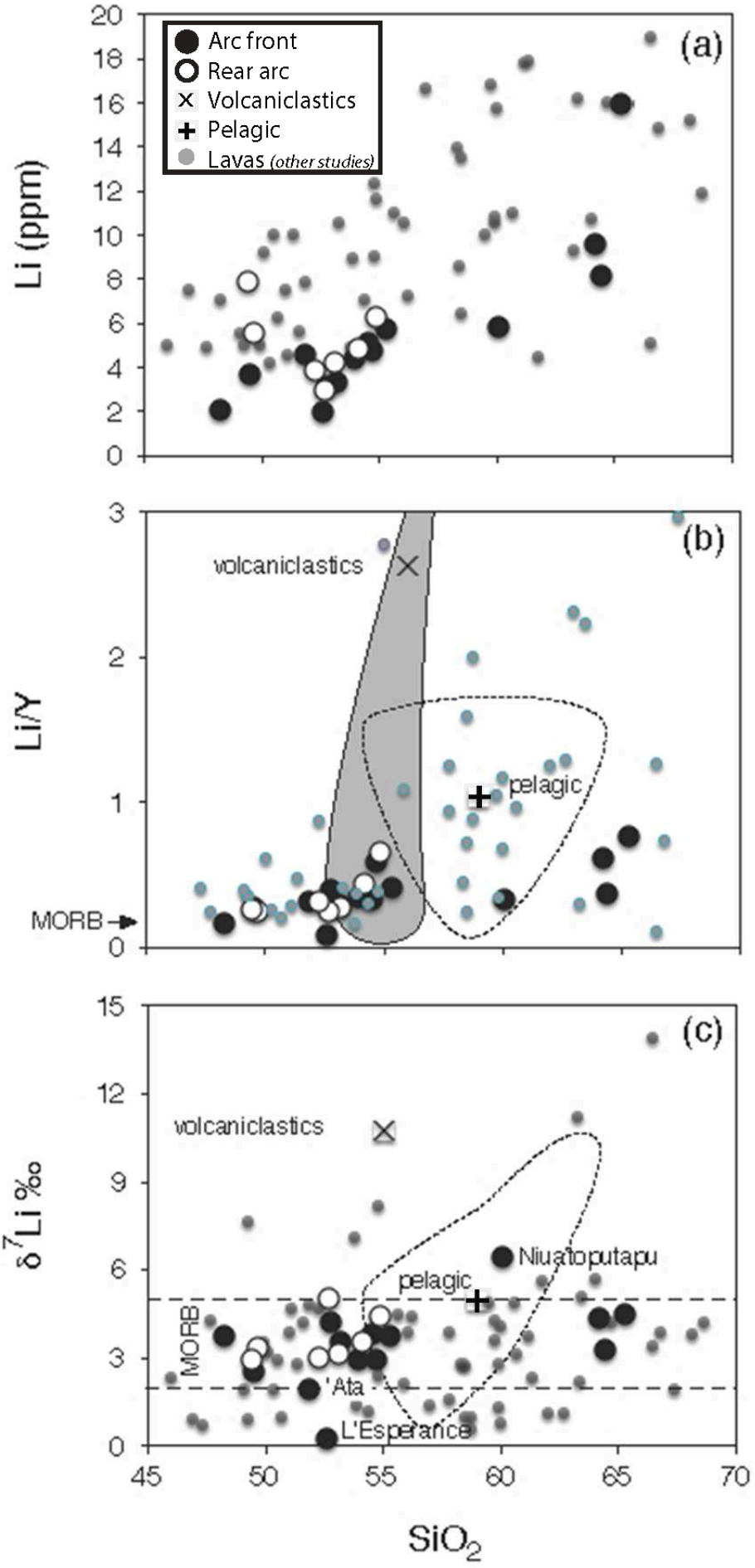

IslandArc_Figure2.png

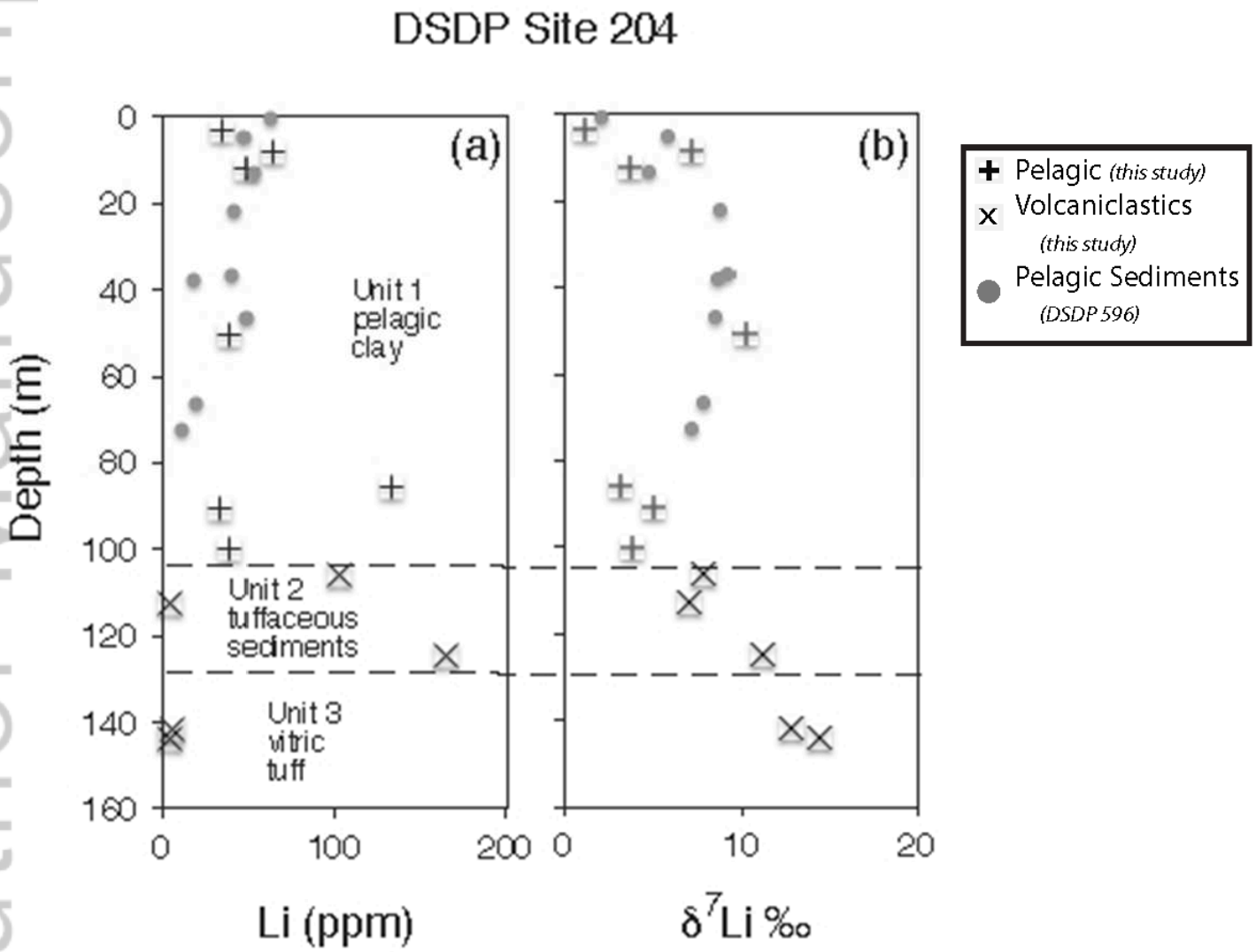

IslandArc_Figure3.png

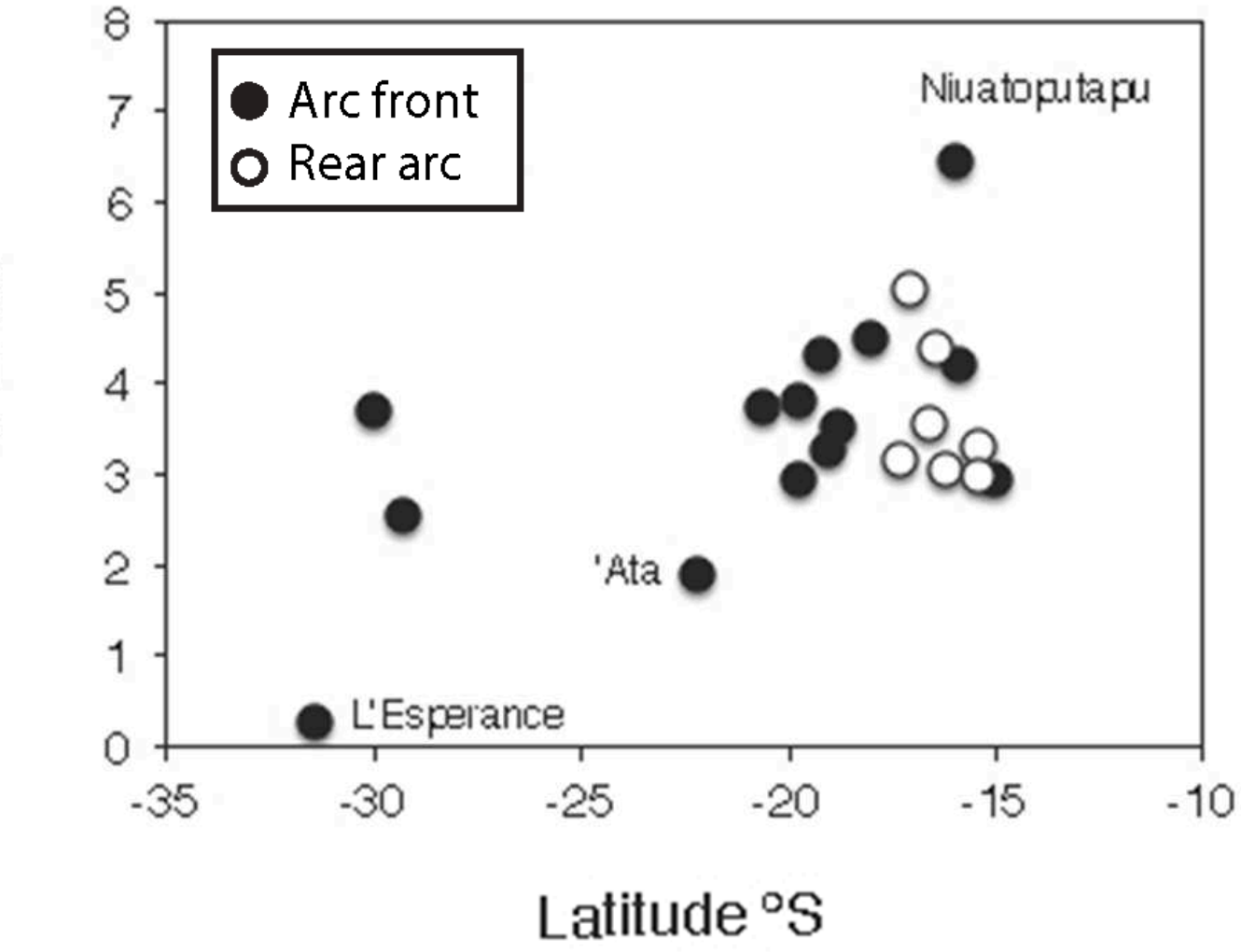

IslandArc_Figure4.png

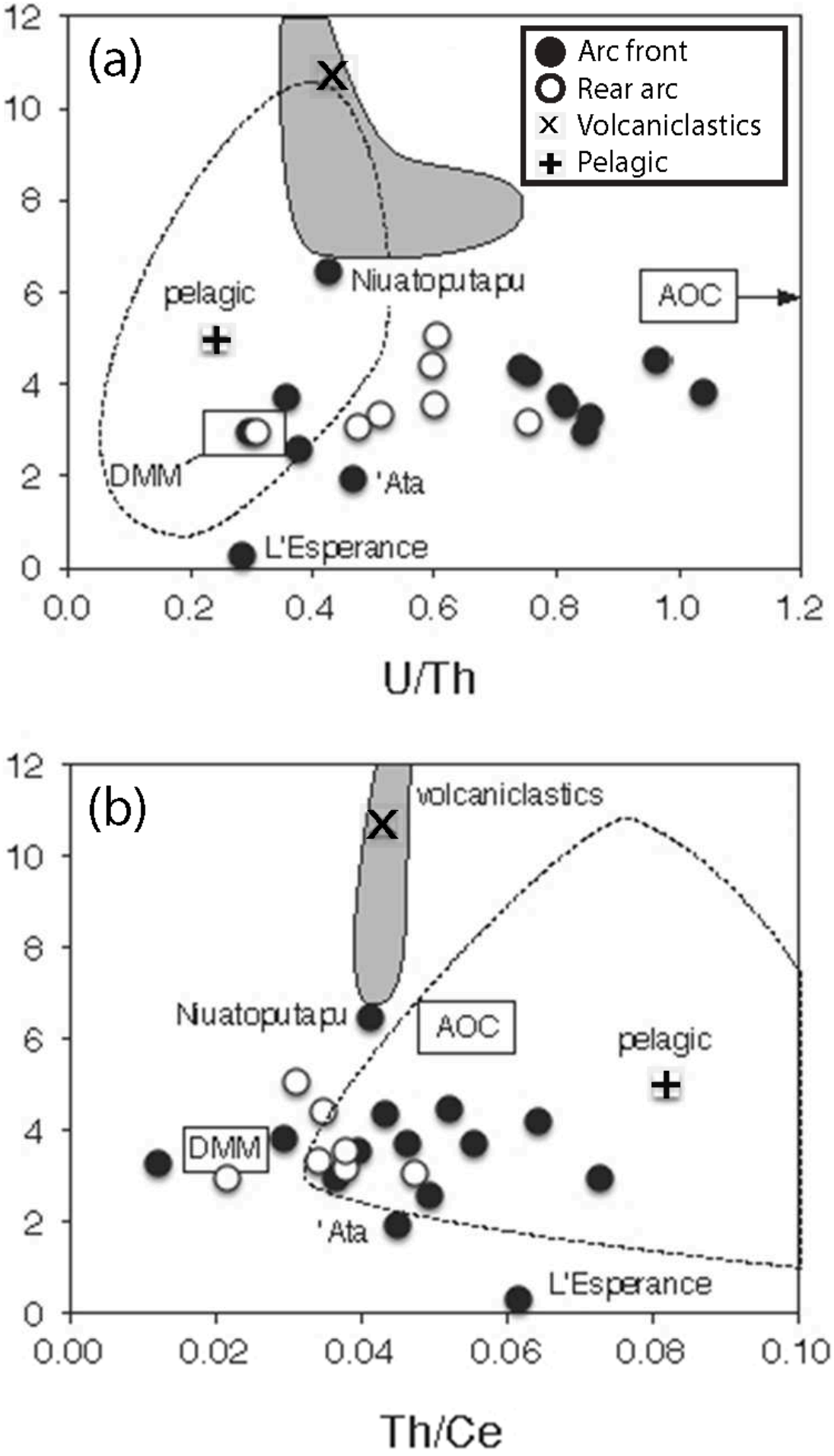

IslandArc_Figure5.png

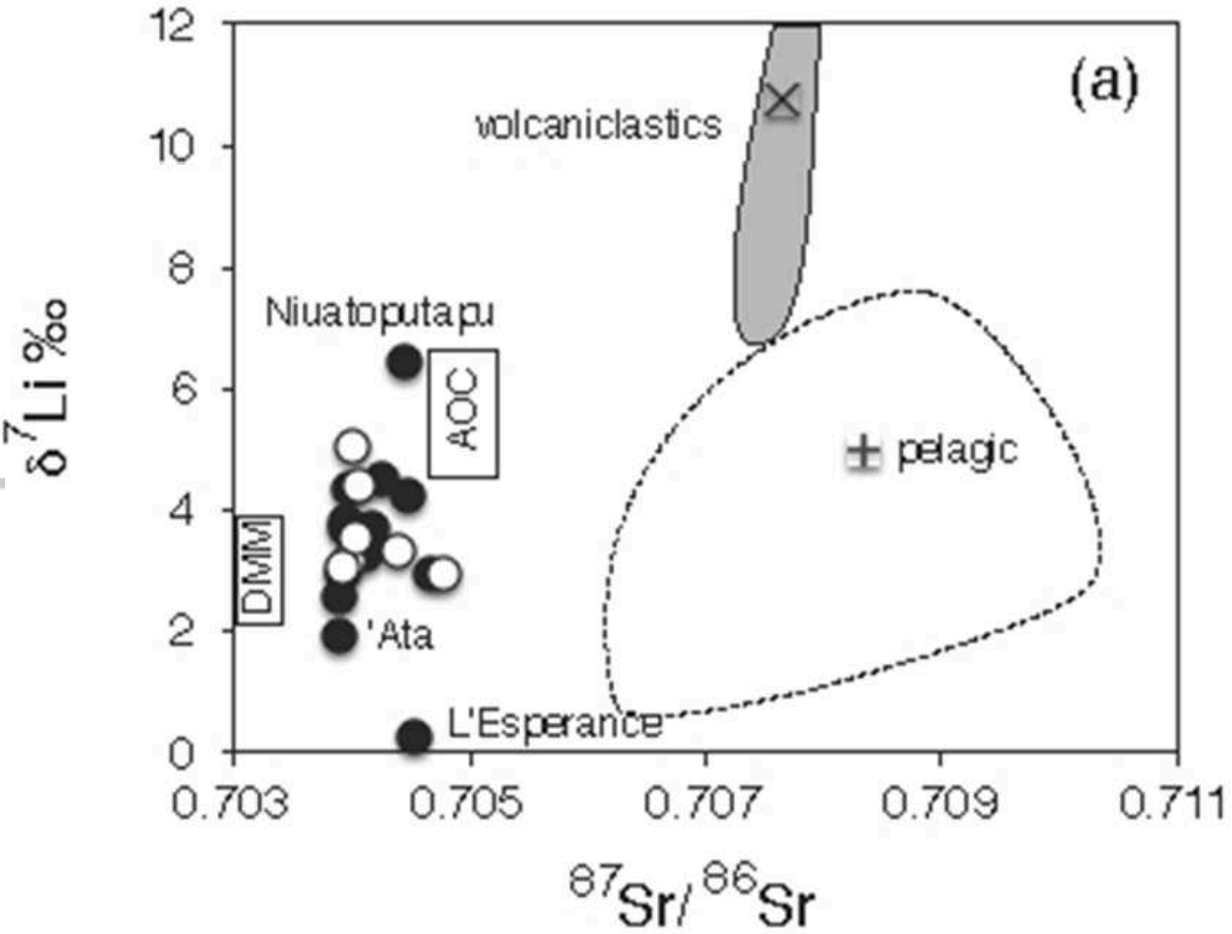

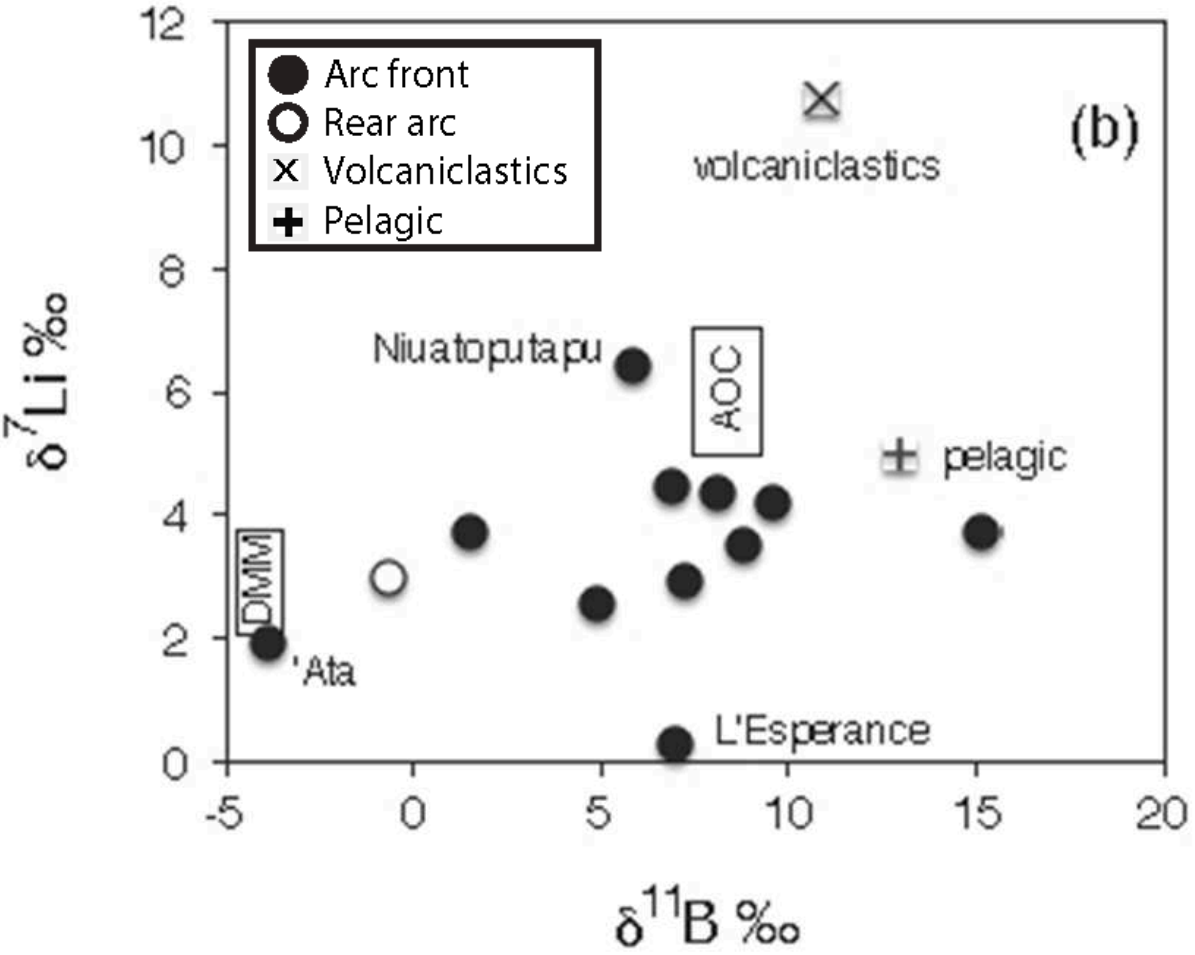

IslandArc_Figure6.png

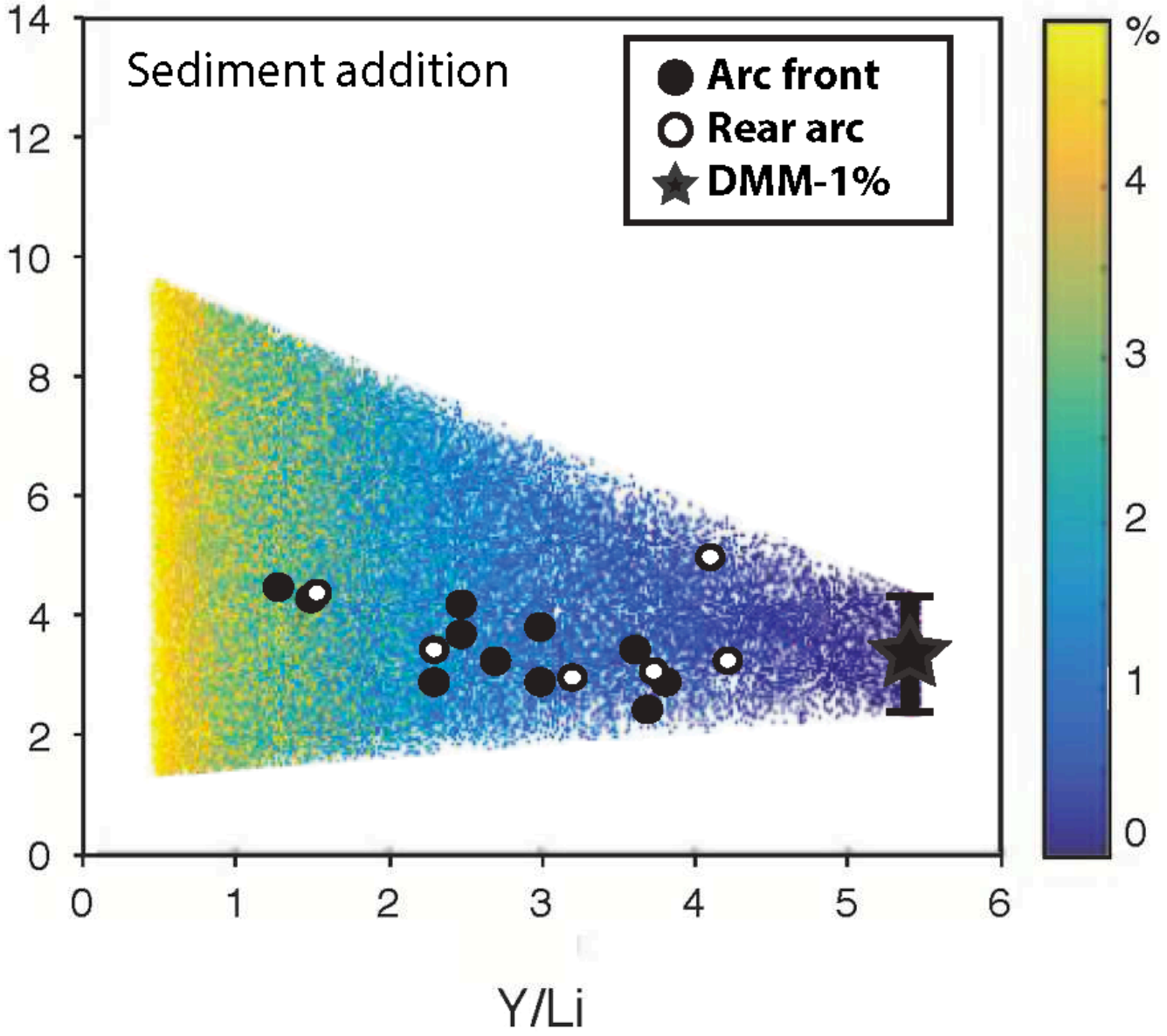

IslandArc_Figure7.png

Table 1. Lithium concentrations and isotope ratios for lavas and standards analysed

Location	Sample ID	SiO_2 (wt. %)	Li (ppm)	δ^7Li (‰)
North Tonga trench	Stn. 25 Boninite	54.72	4.7	2.9
Arc Front Lavas:				
Tafahi	T116	52.81	3.1	4.2
Niuatoputapu	NTT 29/3	60.13	5.8	6.4
Replicate				*7.9*
Fonualei	FON 39	65.34	16.0	4.5
Late	Late 7	53.19	3.3	3.5
Metis Shoal	TLi7	64.25	9.5	4.3
Home Reef	HR06	64.45	8.1	3.3
Tofua	26835	53.94	4.4	2.9
Tofua	26833	54.56	5.0	3.8
Hunga Ha'apai	HHTop	55.35	5.7	3.7
Ata	ATA 8-1	51.90	4.5	1.9
Replicate				*1.6*
Raoul	7125	49.52	3.7	2.5
Macauley	45658	48.30	2.1	3.7
L'Esperance	14831	52.66	1.9	0.3
Back Arc Lavas:				
Fonualei Spreading Centre	ND-46	53.17	4.1	3.1
Fonualei Spreading Centre	ND-40	52.71	2.9	5.0
Fonualei Spreading Centre	ND-58	54.18	4.8	3.5
Fonualei Spreading Centre	ND-61	54.88	6.2	4.4
Fonualei Spreading Centre	ND-67	52.31	3.8	3.0
Mangatolo Triple Junction	ND-69	49.73	5.6	3.3
Niuafo'ou	31461	49.43	7.8	2.9
Standards:	BHVO-2		4.9	3.6
	BHVO-2		4.8	3.2
	AGV-2		11.1	5.2
	AGV-2		10.5	5.6
	BCR-2		10.3	2.1

Table 2. Li concentrations and isotope ratios in DSDP Site 204 Sediments

Sample ID	Type	Depth (m)	Li (ppm)	δ^7Li (‰)
204-1R-3W-60-61	pelagic	3.6	34.5	1.2
204-2R-1W-109-110	pelagic	8.6	64.1	7.3
204-2R-4W-60-61	pelagic	12.6	47.9	3.8
204-3R-2W-59-60	pelagic	50.9	38.8	10.2
204-4R-1W-75-76	pelagic	85.8	133.3	3.2
204-4R-4W-140-141	pelagic	90.9	32.9	5.2
204-5R-4W-60-61	pelagic	100.6	38.8	3.9
204-6R-3W-48-50	volcaniclastic	106.5	102.6	8.0
204-7R-1W-92-93	volcaniclastic	112.9	4.4	7.2
204-8R-3W-86-87	volcaniclastic	124.9	165.3	11.2
204-9R-1W-108-110	volcaniclastic	142.1	5.2	12.8
204-9R-3W-24-27	volcaniclastic	144.2	3.6	14.4